Spectral hole-burning spectroscopy in $Nd^{3+}:YVO_4$

S. R. Hastings-Simon, M. Afzelius, J. Minář, M. U. Staudt, B. Lauritzen, H. de Riedmatten, and N. Gisin
Group of Applied Physics, University of Geneva, CH-1211 Geneva 4, Switzerland

A. Amari, A. Walther, and S. Kröll
Division of Atomic Physics, Lund Institute of Technology, S-221 00 Lund, Sweden

E. Cavalli
Dipartimento di Chimica Generale ed Inorganica, Chimica Analitica e Chimica, Fisica, Università di Parma, Viale G. P. Usberti 17/a, 43100 Parma, Italy

M. Bettinelli
Dipartimento Scientifico e Tecnologico, University of Verona and INSTM, UdR Verona, Strada Le Grazie 15, 37134 Verona, Italy
(Received 24 September 2007; published 10 March 2008)

We present spectral hole-burning measurements on the 879 nm, $^4I_{9/2} \rightarrow {}^4F_{3/2}$ transition in $Nd^{3+}:YVO_4$. We observe antiholes in the spectrum along with long lived spectral holes, which demonstrates optical pumping between the ground state Zeeman levels. The spectral holes are narrow (homogeneous linewidth of 63 kHz) at 2.1 K with a 300 mT applied magnetic field. We also perform preliminary spectral tailoring in this material by creating a 40 MHz wide transmission window in the inhomogeneous absorption. These results show the potential of the Zeeman levels in Nd doped materials to be used for spectral tailoring for quantum and classical information processing.

DOI: 10.1103/PhysRevB.77.125111 PACS number(s): 78.90.+t, 78.47.−p, 61.72.−y, 32.60.+i

I. INTRODUCTION

Rare-earth ion doped solids have been the subject of much investigation in the last decades because of their excellent optical coherence properties.[1] Many applications have been proposed for these materials such as classical data storage by photon echo[2,3] or spectral hole burning,[4] radio frequency spectrum analysis,[5] as well as laser frequency locking.[6] These materials are now also considered for the storage of quantum states carried by single photons, in the context of quantum information science.[7,8] Many protocols for storing single photons in ensembles of atoms have been proposed, e.g., electromagnetically induced transparency[9,10] and photon echo techniques based on controlled reversible inhomogeneous broadening[11–13] (CRIB). Most of the schemes have in common, the need for a level structure with (at least) two long lived ground states that can be efficiently coupled to an excited state via optical transitions, a so-called lambda system. To initialize the memory, it is necessary to be able to efficiently transfer and durably store the population between the ground state levels, for example, using optical pumping via the excited state. For some protocols such as CRIB,[11–13] it is also necessary to be able to tailor the absorption profile, for example, to isolate a narrow absorption peak within a wide transparency window. In this context, several materials have been proposed and investigated as potential materials. Three-level lambda systems with efficient optical pumping have been so far demonstrated in praseodymium,[14–16] europium,[17,18] and thulium[19,20] doped crystals. Population storage in the Zeeman sublevels of $Nd^{3+}:LaF_3$ has also been observed in a different context.[21]

One of the experimental difficulties of implementing a quantum memory with rare-earth ion doped solids is that the optical transitions between the ground state and the excited states typically have small oscillator strengths. Hence, it is difficult to obtain the high optical depths required to achieve efficient storage and retrieval of photonic quantum states.[22–24] Similarly, experiments based on the spontaneous Raman scattering aiming at creating entanglement between atomic ensembles in the solid state[25] require high optical powers, making filtering of the classical beam more challenging. For these reasons, it is interesting to consider rare-earth ions with the highest possible oscillator strength for the optical transition. The most studied systems in this context are the praseodymium doped crystals which have excellent optical and hyperfine coherence times.[15,16] However, these systems have a small separation between hyperfine ground states (a few megahertz). This is a strong limitation for applications that require a large spectral bandwidth. Moreover, the transition used in Pr doped crystals is at a wavelength of 606 nm, where only dye lasers which are difficult to frequency stabilize are available.

In this paper, we investigate experimentally a candidate ion, Nd^{3+}, for quantum storage applications. In general this ion is attractive for quantum and classical information processing because of its $^4I_{9/2} \rightarrow {}^4F_{3/2}$ transition around 880 nm where diode lasers and efficient single photon detectors are available. In addition, Nd^{3+} is a Kramers ion and thus has a strong first-order Zeeman effect which gives a large ground state splitting under the application of a magnetic field (10–100 GHz/T). This large splitting, in turn, translates to a large storage bandwidth for the quantum memory. Recent proposals for quantum repeaters would take advantage of a large storage bandwidth to speed up entanglement distribution.[24] In particular, YVO_4 as a host material for Nd^{3+} ions is of interest because of the high oscillator strength of the ~880 nm transition. Moreover, it has been shown via photon echo measurements that the optical coherence time of

this transition is 20 μs at magnetic fields higher than 1.5 T.[26]

We investigate the 879 nm transition in $Nd^{3+}:YVO_4$ using spectral hole-burning (SHB) techniques[27] and show population storage in the Zeeman levels of the ground state leading to spectral holes that are long lived as compared to the excited-state lifetime. In addition, we demonstrate spectral holes of 125 ± 4 kHz at a temperature of 2.1 K and applied magnetic field of 300 mT. Moreover, we show that it is possible to create a wide (40 MHz) transmission pit in the inhomogeneous absorption profile by optically pumping ions between the Zeeman levels.

II. THEORETICAL BACKGROUND

In SHB spectroscopy[27] of ions with only one ground state and one excited state, an intense laser is used to excite ions from the ground state to the excited state. The population difference can then be probed by attenuating the laser and scanning the frequency around the burning frequency. The ions in the excited state lead to a hole in the inhomogeneous absorption profile manifested as an increase in transmitted light at the corresponding transition wavelength. The width of the hole is limited by the homogenous linewidth of the transition, spectral diffusion, and power broadening.[28]

In the case of an ion with two ground states and two excited states, for instance, corresponding to the Zeeman levels, the spectrum is more complex as the burning frequency can be in resonance with transitions from either of the two ground states to either of the two excited states. These four alternatives correspond to four different classes of ions within the inhomogeneous profile. Ions can be optically pumped via the excited state into the other ground state, leading to an increase in absorption from this other ground state (an antihole). Thus, in addition to the central hole, one expects additional holes as well as antiholes at spacings given by the Zeeman level spacings. Figure 1(a) shows the hole-burning spectrum for one class of ions, the complete spectrum for the four classes is shown in Fig. 1(b).

The YVO_4 crystal is uniaxial, and Nd^{3+} ions substitute for Y^{3+} ions in sites of D_{2d} point symmetry. In a crystal field of this symmetry, the ground state $^4I_{9/2}$ splits into five Kramers doublets, only the lowest being populated at liquid helium temperatures, and the $^4F_{3/2}$ excited state splits into two Kramers doublets. Under an applied magnetic field, the ground and excited-state doublets each split into two Zeeman levels. The optical lifetime of the $^4F_{3/2}$ state has been measured by stimulated photon echo to be 40 μs.[26]

In order to have efficient optical pumping and trapping in the ground state level, it is necessary to have a relaxation time between the ground state levels, which is much longer than the optical T_1 lifetime of the excited state. The signature of storage in the ground state Zeeman levels is the appearance of antiholes at the ground state Zeeman splitting and a central hole with a decay time longer than the excited-state T_1 lifetime.

In SHB experiments, one measures the transmitted intensity after the crystal of length L. The transmitted intensity at position L, $I(L)$, is given by

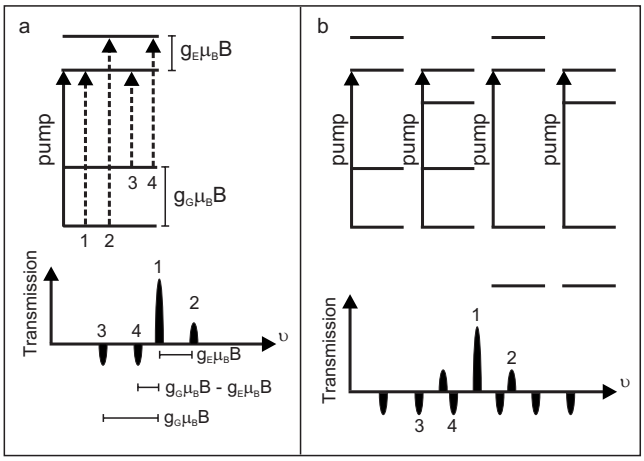

FIG. 1. (a) Four level hole-burning spectrum (Zeeman levels) for the class of ions where the laser is in resonance with the $|g_-\rangle \rightarrow |e_-\rangle$ transition. The g_G (g_E) is the g factor for the ground (excited) state, μ_B is the Bohr magneton, and B is the applied magnetic field. The pump transition (solid line) and possible probe transitions (dashed lines) between the four levels are shown in the energy diagram and labeled on the corresponding transmission spectrum of holes and antiholes. (b) Four level hole-burning spectrum with inhomogeneous broadening. The four different classes of ions within the inhomogeneous profile, which are in resonance with the pump beam, are shown along with the resulting transmission spectrum of holes and antiholes (here, the probe transitions are not shown for clarity).

$$I(L) = I(0)e^{-\alpha L}, \tag{1}$$

where $I(0)$ is the incident intensity and α is the absorption coefficient. The absorption coefficient at a frequency ω is linearly proportional to the population difference, $N_1 - N_2$, where N_1 (N_2) is the number of ions in the ground (excited) state at ω. Therefore, SHB measurements can be used to extract information about the dynamics of the population, in particular, if there is no population in the excited state, then the absorption coefficient is linearly proportional to the ground state population. This is the case for the measurements presented in this paper as the excited-state lifetime is much shorter than waiting time between the spectral hole-burning pulse and the probe pulse. All SHB spectra presented in this paper are the natural logarithm of the measured transmitted intensity.

III. EXPERIMENTAL SETUP AND/OR METHODS

The YVO_4 single crystals doped with Nd^{3+} were grown by spontaneous nucleation from a $Pb_2V_2O_7$ flux.[29] Reagent grade PbO and V_2O_5, Nd_2O_3 (99.99%) and Y_2O_3 (99.99%) were used as starting materials in suitable amounts. The doping concentration was 0.001% (Nd/Y nominal molar ratio). The batch was set in a 50 cm^3 covered platinum crucible and heated to 1300 °C inside a horizontal furnace. After a soaking time of 12 h, the temperature was lowered to 850 °C at a rate of 3–4 °C/h, then the crucible was drawn out from the furnace and quickly inverted to separate the flux from the

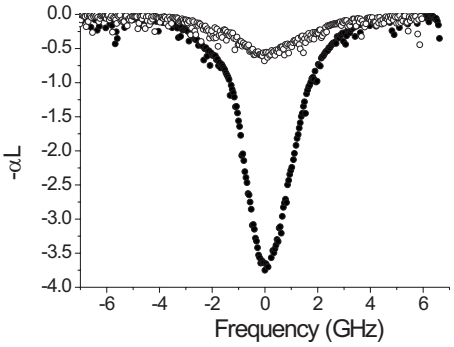

FIG. 2. Absorption as a function of wavelength over the inhomogeneously broadened absorption spectrum of the transmission. The inhomogeneous broadening is roughly 2.1 GHz and the absorption is strongly polarization dependent, with αL of −3.7 for light polarized parallel to the crystal c axis (filled circles) and −0.6 for light polarized perpendicular to the crystal c axis (open circles).

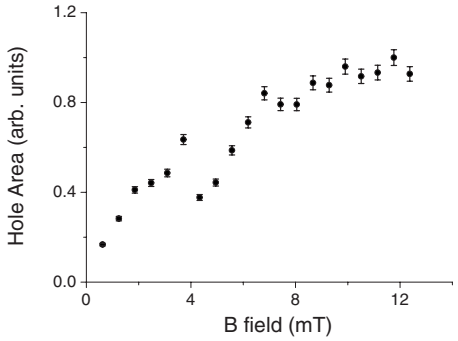

FIG. 3. Area of the central hole 1 ms after spectral hole burning as a function of the applied magnetic field. Here, B was parallel to the c axis with $T=4.2$ K.

crystals grown at the bottom of the crucible. The flux was dissolved by using hot diluted nitric acid. YVO_4 crystallizes in the $I41/amd$ space group, with cell parameters $a=b=7.118$ Å and $c=6.289$ Å and $Z=4$.[30]

The experiments were performed on the 879 nm, $^4I_{9/2} \rightarrow {}^4F_{3/2}$ transition in a $Nd^{3+}:YVO_4$ crystal with a thickness of 0.9 mm along the direction of light propagation, perpendicular to the crystal c axis. Light at 879 nm from a microlase Ti:sapphire laser (MBR-110) in continuous mode with an output power of ~100 mW is modulated by an acousto-optic modulator (AOM) in a double pass setup. By modulating both the amplitude and frequency of the rf wave produced by an arbitrary wave form generator which is used to drive the AOM, we can create pulses and scan the frequency of the light. A $\lambda/2$ plate is used to control the polarization of the light on the sample.

We made measurements in two different cryostats: a He bath cryostat (Cryovac, model 100) with external Helmholtz coils which can produce a magnetic field of up to 15 mT at the sample and a He bath cryostat (Oxford instruments, Spectromag) with a superconducting magnetic that can produce a field of up to 8 T at the sample. The light was focused directly onto the sample in the cryostat and the transmitted light was focused onto a detector (Thorlabs, model PDB150A). A pickoff mirror before the cryostat directed a small percentage of the incident light onto an identical detector to normalize the signal to laser and AOM intensity fluctuations.

IV. RESULTS AND DISCUSSION

A. Spectral hole-burning mechanism

The inhomogeneous absorption spectrum was measured in transmission by slowly scanning the frequency of the Ti:sapphire laser source (see Fig. 2). The inhomogeneous broadening is roughly 2.1 GHz and the absorption is strongly polarized with αL of −3.7 for light polarized parallel to the crystal c axis and −0.6 for light polarized perpendicular to the crystal c axis. The following measurements were performed with the light polarized parallel to the crystal c axis.

For the spectral hole-burning measurements, we used the AOM to create an intense burning pulse. We then probed the spectral hole by scanning the frequency of the AOM around the initial burning frequency using a 1 ms delayed and attenuated read pulse.

We measured the area of the central hole as a function of the applied magnetic field (B parallel to c) at a temperature of 4.2 K, as shown in Fig. 3. Without an applied magnetic field, no or very weak spectral holes were observed. However, under the application of a low magnetic field (a few millitesla), the spectral hole grew very large and saturated at fields of about 10 mT. In general, a spectral hole at the burning frequency can be observed due to population remaining in the excited state or due to ions which are trapped in other ground state levels. In our experiment, where the waiting time between the burning and scan pulses was much longer than the excited-state lifetime (1 ms as compared to 40 μs), there clearly cannot be any contribution to the spectral hole from ions in the excited state. Therefore, the presence of a spectral hole shows that population is trapped in other ground state levels. The strong magnetic field dependence of the hole suggests that population trapping is occurring in the ground state Zeeman levels.

There were also weak holes observed at zero applied magnetic field. These could have several origins. For instance, two isotopes of Nd, ^{143}Nd and ^{145}Nd, naturally occurring at 12.2% and 8.3%, respectively, have a nuclear spin and thus a hyperfine structure in which population could be trapped. In addition, interactions between the nuclear moment of the host ion vanadium and the electronic magnetic moment of Nd^{3+} (superhyperfine interaction) can give rise to additional energy levels where trapping can occur.[31]

B. Homogeneous linewidth

The homogeneous linewidth Γ_h of a transition can be measured directly via spectral hole burning and the spectral hole linewidth Γ_{hole} as $\Gamma_h=\Gamma_{hole}/2$ in the limit where there is no significant spectral diffusion and negligible laser linewidth and power broadening. The homogeneous linewidth has been previously measured to be 15 kHz at a magnetic field higher than 1.5 T using two pulse photon echoes.[26]

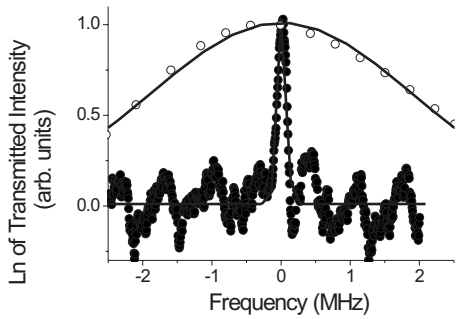

FIG. 4. Spectral hole for applied magnetic fields $B=15$ mT (open circles) and 300 mT (filled circles) parallel to the crystal c axis. Temperature of the sample, $T=2.1$ K. Points are data and lines are a fit to a Gaussian with full widths at half maximum of 3.8 ± 0.2 MHz and 125 ± 4 kHz, respectively.

However, spectral diffusion effects can broaden the hole considerably compared with linewidth values measured via two pulse photon echoes, where the width is measured at a much shorter time scale.[32] The relevant width for a CRIB-based memory is the width of the spectral hole that can be prepared, as the storage time in the excited state is limited to the inverse of the width of the prepared spectral hole.[23]

Spectral holes measured at $T=2.1$ K, for fields $B=15$ and 300 mT parallel to the crystal c axis, are shown in Fig. 4. For an applied field of 15 mT, the spectral hole linewidth is 3.8 ± 0.2 MHz, whereas for an applied field of 300 mT, the spectral hole narrowed significantly to 125 ± 4 kHz, corresponding to Γ_h of 1.9 ± 0.1 MHz and 63 ± 2 kHz, respectively. This is an upper limit on the homogeneous linewidth as we do not take into account the effect of power broadening or the laser linewidth.

The narrow holes at higher field confirm that the width of the spectral hole is reduced with the application of a field which freezes out magnetic interactions as was observed in two pulse photon echo measurements[26] where a Γ_h of 40 kHz was measured for the same applied magnetic field. The fact that via SHB we measure a value that is only slightly larger indicates that spectral diffusion does not play an important role in this sample at 300 mT for the given doping concentration. This was also the conclusion reached by Sun, *et al.*[26] based on a three pulse photon echo experiment.

C. Hole-burning spectrum

For larger frequency scans, one can see the pattern of holes and antiholes expected for a four level system with population trapping in the ground state. In order to characterize the transitions, we measured the spectrum for magnetic fields from 0 to 15 mT for the two inequivalent directions of the magnetic field (B parallel to the c axis and B perpendicular to the c axis). The spectra are shown in Fig. 5.

In the case of B parallel to c, we observe a strong antihole close to the central hole with a relatively small magnetic field dependence, 1.8 MHz/mT [see Figs. 5(a) and 5(b)]. In addition, there are weak hole and antihole with larger magnetic field dependences, 14.8 and 12.9 MHz/mT, respectively. An excited-state Zeeman g factor, $g_E=1.05$, can be extracted from the magnetic field dependence of the weak hole (see Fig. 1), which corresponds well to published values.[33] The g factor of the weak antihole, 0.92, agrees with that of the Zeeman ground state splitting.[33] The magnetic field dependence of the strong antihole corresponds to a g factor of 0.13, which is the difference between our measured g factors for the excited and ground states, as one expects from Fig. 1.

In the case of B perpendicular to c, we observe a strong hole with a magnetic field dependence of 3.92 MHz/mT [see Figs. 5(c) and 5(d)]. There is also a broad and weak antihole structure with a larger magnetic field dependence from which it was not possible to extract a Zeeman g factor. From the strong hole, one can extract an excited-state g factor of 0.28. This value differs from that measured by Mehta *et al.*,[33] 0.18 ± 0.04; however, it is closer to the value of 0.34 which they obtain by crystal field calculations including the Zeeman effect. Note that SHB spectroscopy offers a higher spectral resolution than the fluorescence spectroscopy used in those measurements. The pattern of antiholes at the Zeeman level spacings in Fig. 5, along with the appearance of the central hole at times longer than the excited-state lifetime (Fig. 3) with the application of a magnetic field, confirms that we have population trapping in the Zeeman levels.

D. Zeeman level lifetime

In order to characterize the lifetime of the population trapping, we investigated the dynamics of the central spectral hole. After a burning pulse of 2 ms, we probed the hole with a series of readout pulses of up to 20 ms. In this way, we could measure the decay of the hole as a function of time. We performed this measurement for B parallel to c for temperatures from 1.7 to 4.2 K and magnetic fields from 5 to 15 mT. Over this range, we found no clear dependence of the spectral hole lifetime on the temperature or magnetic field. A typical measurement is shown in Fig. 6 for $T=2.1$ K and $B=5$ mT with a lifetime of 2.1 ± 0.4 ms. We then made a measurement at the higher magnetic field $B=300$ mT (at 2.1 K), as shown in Fig. 6. At this higher field, the lifetime increased to 6 ± 1 ms. Note that we observe an offset in the decay which could be due in part to a long lived component of the spectral hole. This could be due to trapping in hyperfine and superhyperfine levels, as discussed in Sec. IV A.

In the case of Zeeman levels of a paramagnetic ion such as Nd^{3+}, we expect spin lattice relaxation (SLR) to be an important relaxation process. The SLR rate, which is the inverse of the Zeeman state lifetime, has T^9 and B^4 dependences on the temperature and applied magnetic field, respectively.[34–36] Instead, we find no temperature or magnetic field dependence of the lifetime at low fields. A larger applied B field leads to an increase in the lifetime. This indicates that the limiting factor in the lifetime at low fields is not the SLR but rather that the relaxation is driven by interactions which are frozen out by the application of the large magnetic field. This observation is consistent with the behavior of the width of the spectral hole (Fig. 4), which strongly

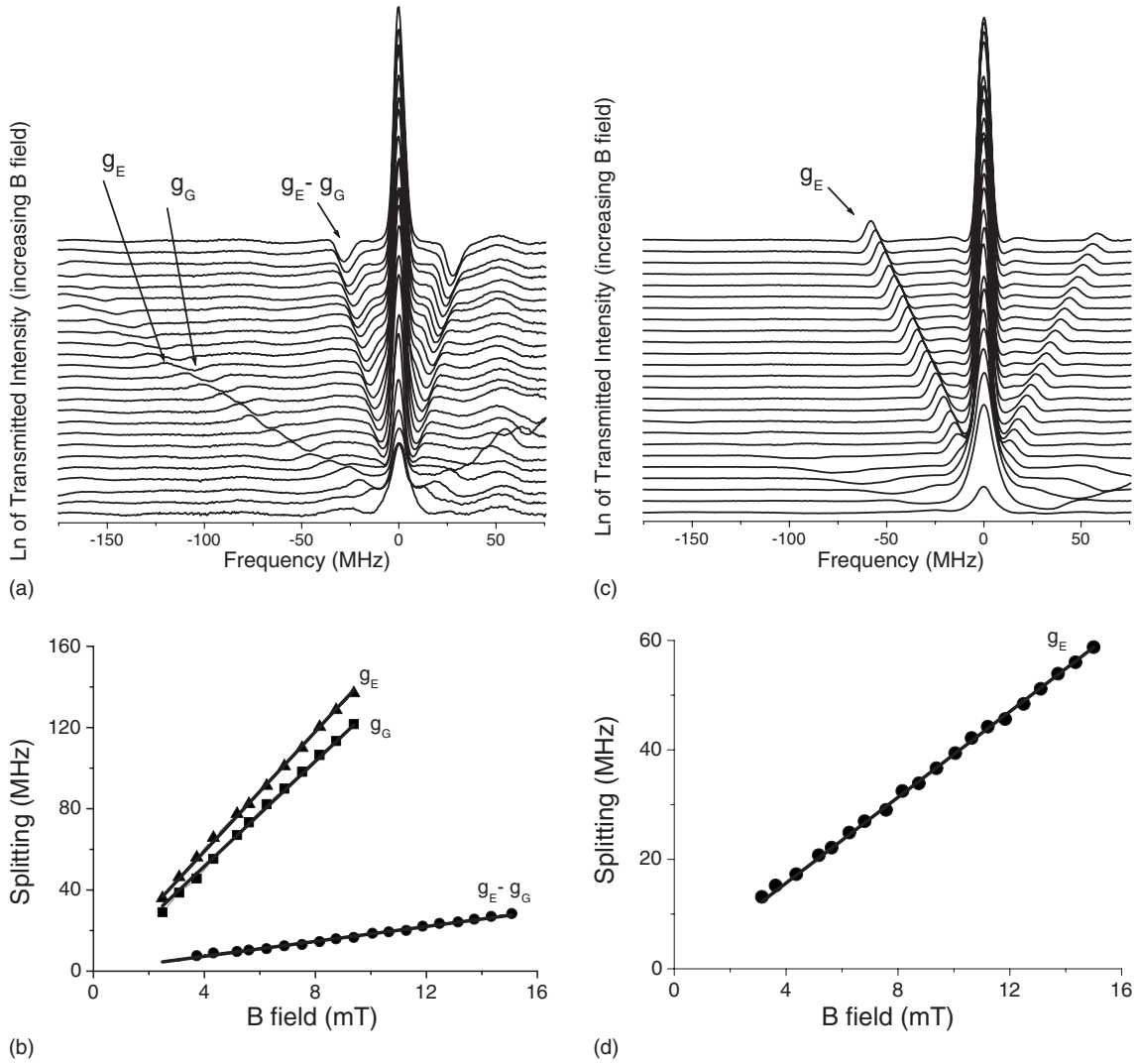

FIG. 5. Transmission spectra for hole burning with (a) $B \| c$ and (c) $B \perp c$. The separation of the holes and antiholes from the central hole as a function of applied field is plotted in (b) for $B \| c$ and (d) for $B \perp c$. The lines are fits to the data and the g values extracted are for $B \| c$, $g_G = 0.92$, $g_E = 1.05$, and $g_E - g_G = 0.13$, and for $B \perp c$, $g_E = 0.28$.

narrows with the larger applied magnetic field. Magnetic spin interactions between neighboring neodymium ions as well as those between neodymium and vanadium ions in the host material are possible sources for the observed Zeeman relaxation. Similar discrepancies between the expected Zeeman lifetime due to SLR and the actual measured lifetime have been reported.[21,37] In general, it appears that the interactions that drive spin relaxations at low magnetic field have not been thoroughly investigated.

E. Spectral tailoring

To measure the percentage of ions trapped and to demonstrate that the Zeeman levels can be used in spectral tailoring of the absorption, we burned a wide transmission pit in the inhomogeneous absorption profile. During a burning time of 10 ms, we made 200 frequency scans of the laser over 40 MHz. Then, after a delay of 10 μs, we reduced the intensity and scanned the laser over 60 MHz in 500 μs to probe the spectrum. The pit burning was done for the case where the burning frequency is in the center of the inhomogeneous

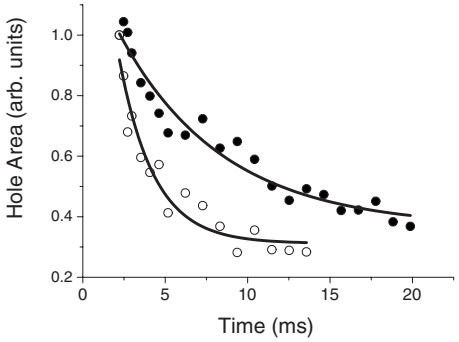

FIG. 6. Area of spectral hole as a function of waiting time at $T = 2.1$ K with applied magnetic fields of 5 mT (open circles) and 300 mT (filled circles). The decay is fit to an exponential with lifetimes of 2.1 ± 0.4 and 6 ± 1 ms, respectively.

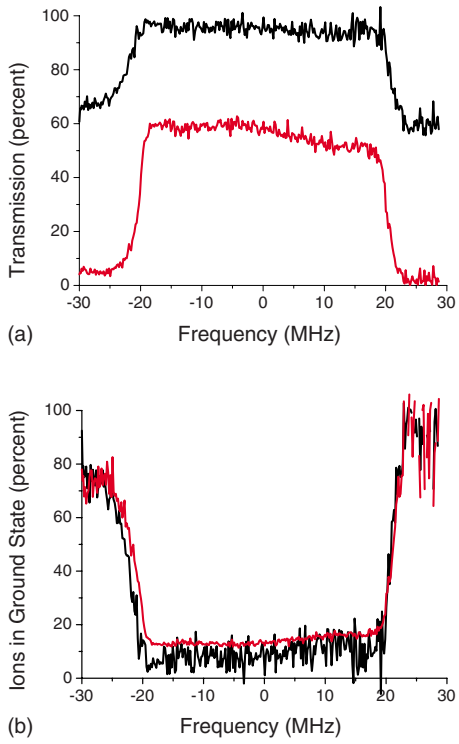

FIG. 7. (Color online) Spectrum after pumping a wide pit in the inhomogeneous absorption profile. (a) Transmission in percentage for two different wavelengths corresponding to initial transmissions of 5% at the center of the inhomogenous profile (red) and 67% off center (black). (b) Percentage of ions that remain in the ground state being probed by the laser, calculated from the data in (a).

broadening where the absorption is largest and toward the edge where there is less absorption. Each measurement was calibrated by tuning the frequency of the laser off resonance and measuring the transmitted light. The transmission pit for the two different initial absorptions is shown in Fig. 7.

In the case of high initial absorption (transmission of about 5%), we achieve a transmission in the pit of roughly 60% after burning [Fig. 7(a)]. For the lower absorption (transmission of about 67%), the transmission rises to ~95% in the pit. In both cases, this corresponds to only 15%–20% of the ions remaining in their initial ground state level [Fig. 7(b)]. Note that there is a slight decrease in transmission at higher frequencies which we mainly attribute to the fact that the scan is 500 μs long compared with a lifetime of the trapping levels of roughly 6 ms.

Given the high ratio of the Zeeman level lifetime (6 ms) to the excited-state lifetime (40 μs), one would expect to trap a much higher percentage than we observed. There could be several explanations for this discrepancy. For instance, this is only true when the pumping rate from the ground to the excited state is of the order of, or faster, than the excited-state relaxation rate. It is also possible for the effective lifetime to be longer than 40 μs because of an unequal branching ratio for changing spin during relaxation. To overcome this limitation, one can increase the excited-state relaxation rate with stimulated emission via an additional energy level, for instance, a crystal field level in the ground state multiplet, using a second laser. It should also be possible to use rf waves to transfer population between excited-state Zeeman levels to improve the branching ratio.

V. CONCLUSION

We have performed spectral hole-burning spectroscopy on the 879 nm, $^4I_{9/2} \rightarrow {}^4F_{3/2}$ transition in $Nd^{3+}:YVO_4$ where we observe strong spectral holes under the application of a small magnetic field. The spectral holes are long lived compared with the excited-state lifetime, indicating the population trapping in the Zeeman sublevels. At low magnetic fields (5–15 mT) and temperatures from 1.7 to 4.2 K, we measure spectral holes of several megahertz and a Zeeman level lifetime of ~2 ms which does not depend on magnetic field or temperatures in this range. In contrast, with a larger applied magnetic field (300 mT), the holes narrow considerably to 125 kHz and the Zeeman level lifetime increases to 6 ms. These results indicate that the dominant relaxation process between the Zeeman levels at low magnetic fields is not spin lattice relaxation as one would expect but a magnetic spin interaction which can be partially frozen out by the application of a moderate magnetic field.

The signatures of the Zeeman level population trapping, antiholes at the ground state splitting difference, and a long lived central hole are clearly observed. We can identify the holes and antiholes due to transitions between the four Zeeman levels of the excited state and the ground state and determine g factors for these levels. In addition, we presented preliminary spectral tailoring results by creating a 40 MHz wide transmission hole in the inhomogeneous absorption.

These results show the potential for the Zeeman levels in Nd^{3+} doped materials to be used to implement a three-level lambda system. The large ratio between the Zeeman level lifetime and the optical T_1 lifetime is promising for efficient pumping and storage. The high absorption ($\alpha \sim 40/\text{cm}$ for $Nd^{3+}:YVO_4$) will allow for a high optical depth, which is necessary for efficient memories, with a relatively short crystal. Moreover, there are other host materials such as $YAlO_3$ (Ref. 38) and Y_2SiO_5 (YSO),[39] where the oscillator strength of the $^4I_{9/2} \rightarrow {}^4F_{3/2}$ transition, while smaller than in YVO_4, is also relatively large as compared with other rare-earth ion transitions. In addition, rare-earth ions doped into YSO have been shown to have good optical coherence properties due to the low nuclear magnetic moments of the host ions.[26] Therefore, we believe that Nd^{3+} doped crystals are interesting for future applications in classical and quantum information processing.

ACKNOWLEDGMENTS

We acknowledge financial support from the Access to Research Infrastructures activity in the Sixth Framework Programme of the EU (Contract No. RII3-CT-2003-506350, Laserlab, Europe), the Swiss NCCR Quantum Photonics, the European Commission under the Integrated Project Qubit Applications (QAP), and the Swedish Research Council (VR).

[1] R. M. Macfarlane, J. Lumin. **100**, 1 (2002).
[2] T. W. Mossberg, Opt. Lett. **7**, 77 (1982).
[3] M. Mitsunaga, Opt. Quantum Electron. **24**, 1137 (1992).
[4] W. E. Moerner, in *Persistent Spectral Hole-Burning: Science and Applications*, edited by W. E. Moerner (Springer, Berlin, 1998).
[5] V. Lavielle, I. Lorger, J. L. Le Gout, S. Tonda, and D. Dolfi, Opt. Lett. **28**, 384 (2003).
[6] T. Bottger, Y. Sun, G. J. Pryde, G. Reinemer, and R. L. Cone, J. Lumin. **94-95**, 565 (2001).
[7] P. Zoller *et al.*, Eur. Phys. J. D **36**, 203 (2005).
[8] *The Physics of Quantum Information: Quantum Cryptography, Quantum Teleportation, Quantum Computation*, edited by D. Bouwmeester, A. K. Ekert, and A. Zeilinger (Springer, Berlin, 2001).
[9] T. Chanelière, D. N. Matsukevich, S. D. Jenkins, S. Y. Lan, T. A. B. Kennedy, and A. Kuzmich, Nature (London) **438**, 833 (2005).
[10] M. D. Eisaman, A. André, F. Massou, M. Fleischhauer, A. S. Zibrov, and M. D. Lukin, Nature (London) **438**, 837 (2005).
[11] S. A. Moiseev and S. Kröll, Phys. Rev. Lett. **87**, 173601 (2001).
[12] B. Kraus, W. Tittel, N. Gisin, M. Nilsson, S. Kroll, and J. I. Cirac, Phys. Rev. A **73**, 020302(R) (2006).
[13] A. L. Alexander, J. J. Longdell, M. J. Sellars, and N. B. Manson, Phys. Rev. Lett. **96**, 043602 (2006).
[14] K. Holliday, M. Croci, E. Vauthey, and U. P. Wild, Phys. Rev. B **47**, 14741 (1993).
[15] M. Nilsson, L. Rippe, S. Kroll, R. Klieber, and D. Suter, Phys. Rev. B **70**, 214116 (2004).
[16] E. Fraval, M. J. Sellars, and J. J. Longdell, Phys. Rev. Lett. **95**, 030506 (2005).
[17] W. R. Babbitt, A. Lezama, and T. W. Mossberg, Phys. Rev. B **39**, 1987 (1989).
[18] M. Nilsson, L. Rippe, N. Ohlsson, T. Christiansson, and S. Kroll, Phys. Scr., T **T102**, 178 (2002).
[19] N. Ohlsson, M. Nilsson, S. Kroll, and R. K. Mohan, Opt. Lett. **28**, 450 (2003).
[20] F. de Seze, A. Louchet, V. Crozatier, I. Lorgeré, F. Bretenaker, J.-L. Le Gouët, O. Guillot-Noël, and P. Goldner, Phys. Rev. B **73**, 085112 (2006).
[21] R. M. Macfarlane and J. C. Vial, Phys. Rev. B **36**, 3511 (1987).
[22] A. V. Gorshkov, A. André, M. Fleischhauer, A. S. Sorensen, and M. D. Lukin, Phys. Rev. Lett. **98**, 123601 (2007).
[23] N. Sangouard, C. Simon, M. Afzelius, and N. Gisin, Phys. Rev. A **75**, 032327 (2007).
[24] C. Simon, H. de Riedmatten, M. Afzelius, N. Sangouard, H. Zbinden, and N. Gisin, Phys. Rev. Lett. **98**, 190503 (2007).
[25] L.-M. Duan, M. D. Lukin, J. I. Cirac, and P. Zoller, Nature (London) **414**, 413 (2001).
[26] Y. Sun, C. W. Thiel, R. L. Cone, R. W. Equall, and R. L. Hutcheson, J. Lumin. **98**, 281 (2002).
[27] R. Macfarlane and R. Shelby, in *Coherent Transients And Hole-burning Spectroscopy In Rare Earth Ions In Solids; Spectroscopy Of Crystals Containing Rare Earth Ions*, edited by A. Kaplyankii and R. Macfarlane (Elsevier Science, Amsterdam, 1987).
[28] E. S. Maniloff, F. R. Graf, H. Gygax, S. B. Altner, S. Bernet, A. Renn, and U. P. Wild, Chem. Phys. **193**, 173 (1995).
[29] G. Garton, S. Smith, and B. M. Wanklyn, J. Cryst. Growth **13-14**, 588 (1972).
[30] B. C. Chakoumakos, M. M. Abraham, and L. A. Boatner, J. Solid State Chem. **109**, 197 (1994).
[31] R. M. Macfarlane, R. S. Meltzer, and B. Z. Malkin, Phys. Rev. B **58**, 5692 (1998).
[32] T. Böttger, C. W. Thiel, Y. Sun, and R. L. Cone, Phys. Rev. B **73**, 075101 (2006).
[33] V. Mehta, O. Guillot-Noel, D. Gourier, Z. Ichalalene, M. Castonguay, and S. Jandl, J. Phys.: Condens. Matter **12**, 7149 (2000).
[34] D. A. Davids and P. E. Wagner, Phys. Rev. Lett. **12**, 141 (1964).
[35] G. H. Larson and C. D. Jeffries, Phys. Rev. **141**, 461 (1966).
[36] I. Kurkin and K. Chernov, Physica B & C **101**, 233 (1980).
[37] S. R. Hastings-Simon, B. Lauritzen, M. U. Staudt, M. Afzelius, H. de Riedmatten, and N. Gisin (unpublished).
[38] M. J. Weber and T. E. Varitimos, J. Appl. Phys. **42**, 4996 (1971).
[39] R. Beach, M. D. Shinn, L. Davis, R. W. Solarz, and W. F. Krupke, IEEE J. Quantum Electron. **26**, 1405 (1990).